Adaptive Shifts in Gene Regulation Underlie a Developmental Delay in Thermogenesis in High-Altitude Deer Mice

Jonathan P. Velotta [1],*[,1] Cayleih E. Robertson,[2] Rena M. Schweizer,[1] Grant B. McClelland [2],[2] and Zachary A. Cheviron[1]

[1]Division of Biological Sciences, University of Montana, Missoula, MT

[2]Department of Biology, McMaster University, Hamilton, ON, Canada

*Corresponding author: E-mail: jonathan.velotta@gmail.com.

Associate editor: Ilya Ruvinsky

Abstract

Aerobic performance is tied to fitness as it influences an animal's ability to find food, escape predators, or survive extreme conditions. At high altitude, where low O_2 availability and persistent cold prevail, maximum metabolic heat production (thermogenesis) is an aerobic performance trait that is closely linked to survival. Understanding how thermogenesis evolves to enhance survival at high altitude will yield insight into the links between physiology, performance, and fitness. Recent work in deer mice (*Peromyscus maniculatus*) has shown that adult mice native to high altitude have higher thermogenic capacities under hypoxia compared with lowland conspecifics, but that developing high-altitude pups delay the onset of thermogenesis. This finding suggests that natural selection on thermogenic capacity varies across life stages. To determine the mechanistic cause of this ontogenetic delay, we analyzed the transcriptomes of thermoeffector organs—brown adipose tissue and skeletal muscle—in developing deer mice native to low and high altitude. We demonstrate that the developmental delay in thermogenesis is associated with adaptive shifts in the expression of genes involved in nervous system development, fuel/O_2 supply, and oxidative metabolism pathways. Our results demonstrate that selection has modified the developmental trajectory of the thermoregulatory system at high altitude and has done so by acting on the regulatory systems that control the maturation of thermoeffector tissues. We suggest that the cold and hypoxic conditions of high altitude force a resource allocation tradeoff, whereby limited energy is allocated to developmental processes such as growth, versus active thermogenesis, during early development.

Key words: **thermogenic capacity, WGCNA, gene expression, *Peromyscus*, high elevation, thermoregulation.**

Introduction

Fitness in the wild is determined by suites of interacting traits that influence variation in whole-organism performance. Performance in turn determines an organism's ability to conduct ecologically relevant tasks such as avoiding predators, competing for resources, and surviving extreme events (Huey and Stevenson 1979; Garland and Losos 1994; Irschick and Garland 2001; Irschick et al. 2008; Campbell-Staton et al. 2017). Many of these ecologically relevant tasks that impinge on whole-organism performance are ultimately dependent on the capacity for aerobic metabolism, and thus, the ability to transport and utilize O_2. As such, the development of the physiological machinery needed to deliver O_2 and metabolize fuels is closely tied to both postnatal juvenile survival and the future reproductive success as adults. The timing of key developmental events and responses to early environmental exposures should therefore influence the evolution of whole-organism performance (Lailvaux and Husak 2014). Studies that seek to understand how performance evolves in the context of development are rare but are needed to determine the causal connections between phenotype and fitness in the wild.

Extreme environments, such as high-altitude habitats >3,000 m above sea level (a.s.l.; Bouverot 1985), are windows into the mechanisms that shape adaptive variation in performance, since the selection pressures are few in number and strong in magnitude (Garland and Carter 1994). The agents of selection at high altitude—cold temperature and unavoidable reductions in available O_2 (hypobaric hypoxia)—have led to clear examples of local adaptation in animals that live there permanently (e.g., Beall 2007; Storz et al. 2010; Simonson et al. 2012). A considerable amount of recent work on high-altitude adaptation has been conducted on the North American deer mouse (*Peromyscus maniculatus*) owing to its broad altitudinal distribution, ranging from sea level to >4,000 m a.s.l. (King 1968). Recent comparative physiological work demonstrates that adult high-altitude deer mice from the Colorado Rocky Mountains have consistently higher aerobic performance capabilities than conspecifics in the Great Plains: High-altitude deer mice are capable of greater aerobic performance under hypoxia and in response to extreme cold (referred to as thermogenic capacity) measured in the wild and in the laboratory (Cheviron et al. 2012, 2013, 2014; Lui et al. 2015; Lau et al. 2017; Tate et al. 2017). Capture–mark–recapture data confirm that higher thermogenic capacities

Article

are beneficial for survival at high altitude (Hayes and O'Connor 1999). These data suggest that enhanced thermogenic capacity provides an important performance benefit in high-altitude deer mice that is strongly tied to fitness during adulthood.

Recent work has uncovered the factors that shape adaptive variation in thermogenic performance to illuminate links between physiology and fitness. This research, conducted in adult deer mice, suggests that improved thermogenic performance is related to alterations to O_2 transport and utilization, including more effective breathing patterns (Ivy and Scott 2017), higher blood-O_2 affinity (Snyder 1981; Snyder et al. 1982; Chappell and Snyder 1984; Storz 2007, 2016) and circulation (Tate et al. 2017), an improved capacity to oxidize lipids as fuel (Cheviron et al. 2012, 2014), and a greater oxidative capacity in skeletal muscles and their mitochondria (Lui et al. 2015; Scott et al. 2015; Mahalingam et al. 2017). Despite the importance of these changes in adults, it is not clear how high-altitude animals have evolved to survive the unique challenges of cold and hypoxic stress during development. Early postnatal development, however, is critically linked to fitness: Altricial rodent pups are small, immobile, and reliant on limited energy supplied through maternal care, and pup mortality can be extremely high in the wild (Hill 1983). Moreover, mouse pups are not born with the ability to generate heat (Pembrey 1895). Independent thermogenic abilities develop as a result of the maturation of two thermoeffector organs, brown adipose tissue (BAT) and skeletal muscle, which permits nonshivering thermogenesis (NST) and shivering thermogenesis, respectively (Lagerspetz 1966; Arjamaa and Lagerspetz 1979). Accordingly, if selection pressures on thermogenic performance are constant across life stages, then thermogenesis should develop faster in high-altitude pups to support an improved adult performance.

However, Robertson et al. (2019) have recently demonstrated that NST is delayed by ~2 days in high-altitude deer mouse pups compared with lowland conspecifics and a closely related, but strictly lowland species, *Peromyscus leucopus*. This delay in the onset of NST is further associated with a delay in the onset of shivering thermogenesis until the normal date of weaning (Robertson and McClelland 2019; fig. 1). The authors suggest that the observed ontogenetic delay may be an evolutionary response to limitations in energy production or allocation at high altitude (e.g., as a result of low O_2), which forces a tradeoff between active thermogenesis and other developmental functions such as growth. Consistent with this interpretation, growth rates under common garden conditions are identical between low- and high-altitude pups, despite the fact that high-altitude mothers produce larger litters (Robertson et al. 2019).

We tested the hypothesis that the ontogenetic delay in thermogenesis is driven by gene regulatory changes that delay the development of the primary thermoeffector organs. To do this, we compared BAT and skeletal muscle transcriptomes in deer mice native with low and high altitudes across the first 27 days of life. We associated variation in transcript abundances to variation in thermogenic capabilities using a gene coexpression network approach that has been used to link gene regulation to physiological function in variety of evolutionary contexts (DeBiasse and Kelly 2016; Velotta et al. 2016, 2018; Campbell-Staton et al. 2018). We show that the delay in thermogenesis in high-altitude mice is associated with a delay in the expression of gene networks that function in nervous system control of BAT, fuel/O_2 supply to BAT, as well as aerobic metabolism and mitochondrial biogenesis in skeletal muscle. Finally, using a combination of phenotypic divergence and population-genetic approaches, we provide evidence that the ontogenetic delays in thermogenesis and their associated regulatory changes are adaptive at high altitude. By combining these approaches, we demonstrate, for the first time, that selection has altered the developmental trajectories of a thermoregulatory system by acting on the regulatory control of thermoeffector organ phenotype.

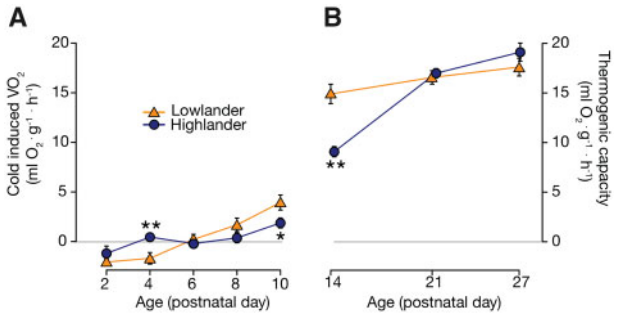

FIG. 1. The development of thermogenesis is delayed in highland (blue, circles) relative to lowland (orange, triangles) deer mice. (*A*) Cold (24 °C)-induced O_2 consumption rate (VO_2) across postnatal day p2–p10. Values constitute the difference between cold-induced and normothermic VO_2, which controls for the stress of separating pups from their mothers at a young age. Values crossing zero indicate that pups are able to generate heat independently. (*B*) Thermogenic capacity (VO_2 max during exposure to 5 °C in heliox) under normoxia is significantly lower in highlanders than lowlanders at p14. Values represent mean mass-corrected VO_2. *$P < 0.05$ and **$P < 0.01$. Data from Robertson et al. (2019) (*A*) and Robertson and McClelland (2019) (*B*).

Results

The Ontogeny of Thermogenesis

We reanalyzed cold-induced metabolic rate (rates of O_2 consumption, VO_2) from Robertson et al. (2019) and Robertson and McClelland (2019) to assess the ontogeny of thermogenesis in deer mice native to lowland (320 m a.s.l.) and highland (4,350 m a.s.l.) habitats. VO_2 of pups postnatal age p0–p10 was measured during exposure to a mild cold stressor (24 °C) and was calculated as the difference in cold-induced VO_2 compared with that of normothermic (30 °C) littermates (see Materials and Methods). Cold-induced VO_2 in these young pups was ~0 until p6 for highlanders and lowlanders (fig. 1A). After p6, cold-induced VO_2 increased in both populations but did so at a slower rate in highlanders (fig. 1). Statistically significant population differences in VO_2 were detected at p4 and p10 (fig. 1). We measured thermogenic capacity in older pups (age p14, p21, and p27) as VO_2max during exposure to cold (−5 °C) in a heliox air mixture.

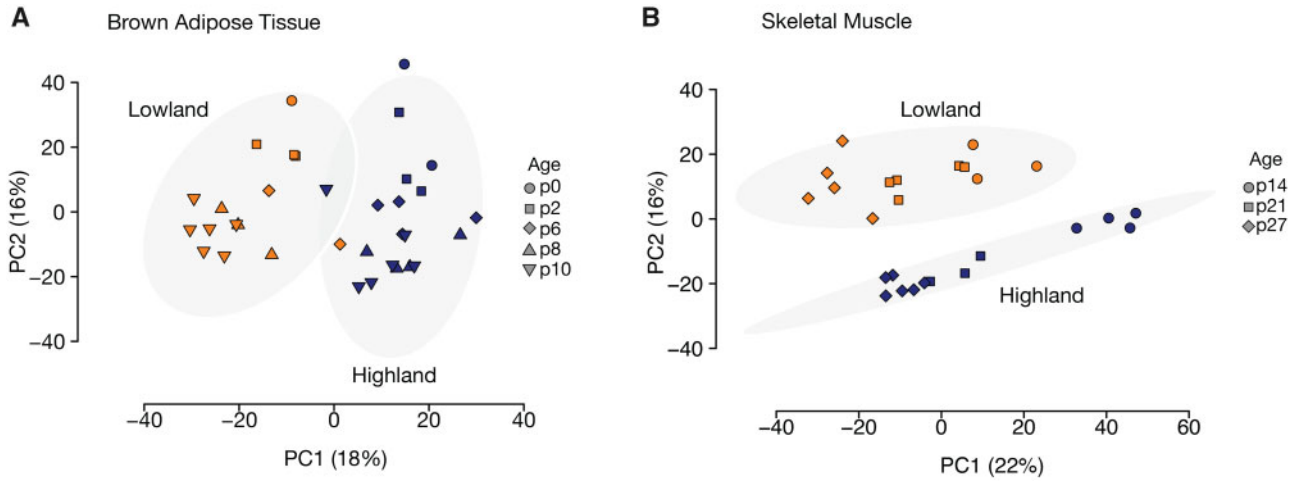

Fig. 2. PCA of transcriptome expression data for thermoeffector organs (*A*) BAT and (*B*) skeletal muscle in lowland (orange points) and highland (blue points) deer mice. Symbols represents ages from postnatal day p0–p10 for BAT, and p14–p27 in skeletal muscle. Populations separated along PC1 in BAT data and PC2 in skeletal muscle data. Gray circles are 95% confidence ellipses drawn around each population to highlight separation.

Table 1. BAT Modules Significantly Correlated with Cold-Induced VO_2.

Module	Module Size	Population		Age		Pop × Age		VO_2 Correlation	
		$F_{1,30}$	*P*	$F_{1,30}$	*P*	$F_{1,30}$	*P*	*r*	*P*
B2	1,022	7.4	0.41	3.2	1.0	5.36	1.0	−0.49	*0.02*
B3	773	27.0	*<0.001*	20.8	*<0.001*	1.67	1.0	0.67	*<0.001*
B4	252	18.6	*0.01*	38.1	*<0.001*	0.43	1.0	−0.56	*0.004*
B11	99	162.1	*<0.001*	26.8	*<0.001*	0.04	1.0	−0.47	*0.02*
B12	605	21.5	*<0.001*	128.2	*<0.001*	4.90	1.0	−0.81	*<0.001*
B16	149	2.7	1.0	25.9	*<0.001*	0.06	1.0	−0.55	*0.01*
B32	267	0.1	1.0	32.9	*<0.001*	0.36	1.0	−0.52	*0.01*
B33	1,073	0.7	1.0	53.9	*<0.001*	0.85	1.0	0.64	*<0.001*
B35	74	37.3	*<0.001*	0.9	1.0	0.02	1.0	−0.45	*0.03*
B36	708	26.5	*<0.001*	51.5	*<0.001*	1.52	1.0	0.58	*<0.001*

Note.—Full association test results are presented in supplementary table S3, Supplementary Material online. Effect of population (highland vs. lowland), age (postnatal day p0–p10), or their interaction from ANOVA models on rank-transformed module expression values (module eigengene). Final two columns present results of Pearson correlation between module eigengene and cold-induced VO_2. *P* values from association tests and ANOVAs were corrected for multiple testing using the false-discovery rate method. Significant *P*-values are italicized.

Highland deer mice exhibited a significantly reduced thermogenic capacity at p14 compared with lowlanders (~6 ml O_2 per gram per hour, on average), whereas by p21 thermogenic capacities between populations were nearly equivalent (fig. 1*B*). Although there is a trend toward highlanders surpassing lowlanders by p27, this was not statistically significant ($P = 0.2$).

Transcriptional Correlates of Thermogenesis

We sequenced the transcriptomes of two thermoeffector organs, BAT and skeletal muscle, in order to assess regulatory mechanisms underlying evolutionary change in the ontogeny of thermogenesis at high altitude. Principal components analysis (PCA) of transcriptome-wide patterns of gene expression revealed separation between lowlanders and highlanders, and across ontogeny, in BAT and skeletal muscle (fig. 2). For BAT, highlanders and lowlanders were distinguishable along PC1, which explained 18% of total variation in expression. By contrast, PC2, which explained 16% of the variance, distinguished postnatal age (fig. 2*A*). We observed similar separations in skeletal muscle samples, although in this case populations were distinguishable along PC1 (22% of variance), and postnatal age distinguishable along PC2 (16% of variance). Ninety-five percent confidence ellipses were drawn around each population demonstrating that populations were entirely (skeletal muscle, fig. 2*B*) or almost entirely (BAT, fig. 2*A*) nonoverlapping in PC1 and PC2 space.

Weighted gene coexpression network analysis (WGCNA) of BAT samples across p0–p10 yielded 38 modules ranging in size from 61 to 1,073 genes (see supplementary table S2, Supplementary Material online, for a full list of module assignments). A total of 1,588 out of 11,192 genes could not be assigned to any module (module B0). We found ten modules exhibiting statistically significant associations between module eigengene and cold-induced VO_2, after correction for multiple testing (table 1). Of the ten VO_2-associated modules, six exhibited significant population effects on module eigengene (table 1). Two of these (modules B11 and B35) were not significantly enriched for Gene Ontology (GO) terms or were enriched for terms unrelated to thermogenesis (e.g., "drug

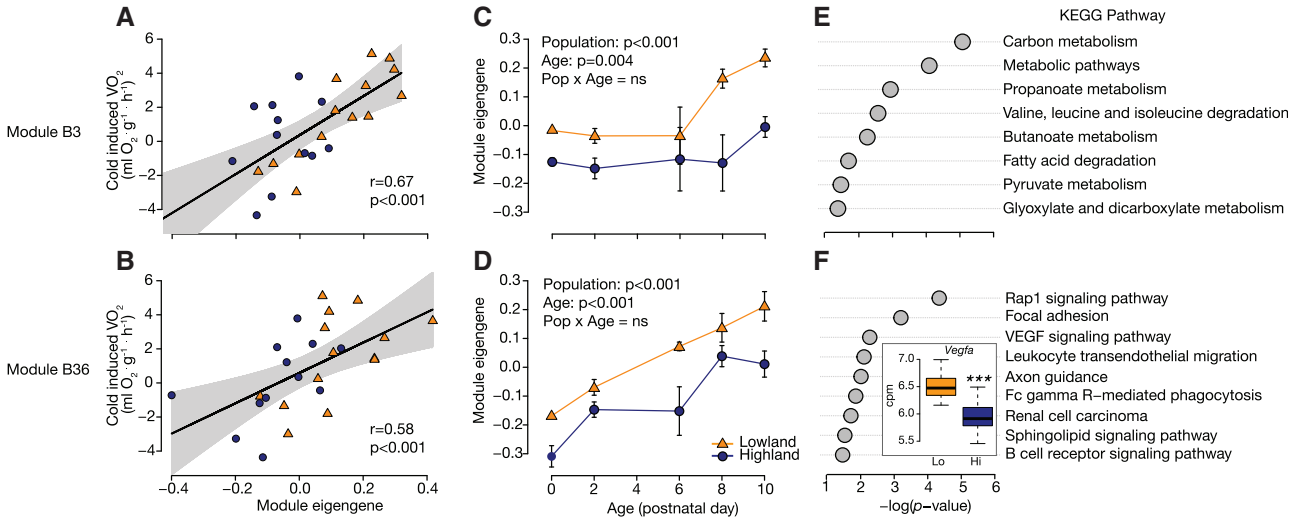

Fig. 3. Two BAT modules are associated with variation in thermogenesis in p0–p10 deer mouse pups. (*A*, *B*) The significant positive association between module eigengene and cold-induced VO_2 (measure of thermogenesis). Eigengene values of modules B3 (*C*) and B36 (*D*) are significantly affected by age, and significantly differentiated between lowland (orange, triangles) and highland (blue, circles) populations. We detected significant enrichment of KEGG pathways related to metabolism and fatty acid degradation in B3 (*E*), and VEGF signaling and axon guidance in B36, among others (*F*). Values in (*E*, *F*) are the negative log of the enrichment test *P* value after correction for multiple testing using the g:SCS algorithm in *gProfilerR* (Reimand et al. 2016). Inset in (*F*) shows average expression (log counts per million; cpm) across age for *Vegfa* in lowlanders (orange) versus highlanders (blue). ***$P < 0.001$. See supplementary table S4, Supplementary Material online, for full functional enrichment analysis results.

metabolism"; see supplementary table S4, Supplementary Material online, for the full list of enriched terms). Modules B4 and B12 (table 1) were both significantly enriched for genes that encode ribosomal proteins (supplementary table S4, Supplementary Material online), which may indicate differences in protein translation between populations. No significant interaction effects were detected for any VO_2-associated module (table 1).

Modules B3 and B36, by contrast, were positively associated with cold-induced VO_2 (fig. 3*A* and *B*), expressed at significantly lower levels in highlanders compared to lowlanders (fig. 3*B* and *C*), and exhibited significant enrichment for functions that reflect a delay in the development of BAT in highlanders (fig. 3*E* and *F*). Module B3 was enriched for functional terms related to fatty acid metabolism in the mitochondria, including the GO Biological Process term "fatty acid metabolic process," the GO Cellular Component term "mitochondron," the KEGG pathway "fatty acid degradation" (fig. 3*E*), and Reactome and WikiPathways terms "fatty acid metabolism" and "fatty acid beta oxidation" (supplementary table S4, Supplementary Material online). Module B36 was enriched for terms related to the vascularization of BAT and the development of its neural circuitry (fig. 3*F*): vascularization terms include the GO Biological Processes "blood vessel development" and "vasculature development," as well as the KEGG pathway "vasculature endothelial growth factor (VEGF) signaling," which is the major pathway regulating new blood vessel growth. Indeed, *Vegfa* exhibits significantly lowered expression in highland compared with lowland mice (fig. 3*F* inset), though it was not assigned to module B36 (supplementary table S2, Supplementary Material online). Finally, we detected enrichment of the KEGG pathway "axon guidance," which represents a key stage in the development of neuronal networks.

We performed WGCNA on skeletal muscle transcriptomes from lowland and highland deer mice sampled at postnatal days 14, 21, and 27. WGCNA identified seven modules ranging in size from 92 to 2,878 genes (table 2). A total of 3,529 out of 11,104 genes could not be assigned to any module (M0; supplementary table S2, Supplementary Material online). Although individual-level thermogenic capacity data do not exist for the samples sequenced, we did detect significant correlations between module eigengene and thermogenic capacity at the level of population and age for two modules, M2 ($r = -0.94$; $P = 0.006$) and M6 ($r = 0.98$; $P < 0.001$; fig. 4*A* and table 2). Despite the fact that we detected an overall effect of postnatal age, but not population, on both of these modules (table 2), expression followed a pattern that closely resembled population-level variation in thermogenic capacity. For module M6 in particular, as with thermogenic capacity (fig. 1*B*), expression was lower in highland compared with lowland deer mice at p14 ($F_{1,4} = 27.7$; $P = 0.006$), but no different from lowlanders at p21 ($F_{1,5} = 0.6$; $P < 0.05$) or p27 ($F_{1,6} = 0.6$; $P > 0.05$; fig. 4*B*). The opposite was true of M2, whereby module expression at p14 was significantly higher in high-altitude mice ($F_{1,4} = 27.7$; $P = 0.02$).

Functional enrichment analysis of VO_2-associated skeletal muscle modules revealed enrichment of a wide variety of biological functions (supplementary table S4, Supplementary Material online). Module M2 for example was enriched for pathways that function in the development of muscle blood supply, including the GO Biological Process terms "angiogenesis, blood vessel morphogenesis, and vasculogenesis." This result may reflect an initiation of blood

Table 2. Association Test and ANOVA Results on Skeletal Muscle Modules.

Module	Module Size	Population		Age		Pop × Age		VO_2 Correlation	
		$F_{1,22}$	*P*	$F_{1,22}$	*P*	$F_{1,22}$	*P*	*r*	*P*
M1	92	3.4	0.6	15.0	*0.006*	2.4	1	0.18	0.99
M2	2,654	1.0	1	150.5	*<0.001*	0.3	1	−0.94	*0.02*
M3	1,052	11.9	*0.02*	1.8	1	2.3	1	−0.79	0.15
M4	288	97.8	*<0.001*	8.7	*0.06*	1.7	1	0.0002	0.99
M5	168	4.6	0.4	3.5	0.61	4.4	0.4	0.19	0.99
M6	2,878	3.2	0.7	64.4	*<0.001*	0.1	1	0.98	*0.004*
M7	443	91.1	*<0.001*	7.2	0.11	1.0	1	0.07	0.99

NOTE.—Effect of population (highland vs. lowland), age (postnatal day p14–p27), or their interaction on rank-transformed module expression (module eigengene values) is presented. Final two columns present results of Pearson correlation between module eigengene and thermogenic capacity. Note that correlations were performed on population-age means since VO_2 measurements did not exist for the individuals sequenced. *P* values from association tests and ANOVAs were corrected for multiple testing using the false-discovery rate method. Significant *P*-values are italicized.

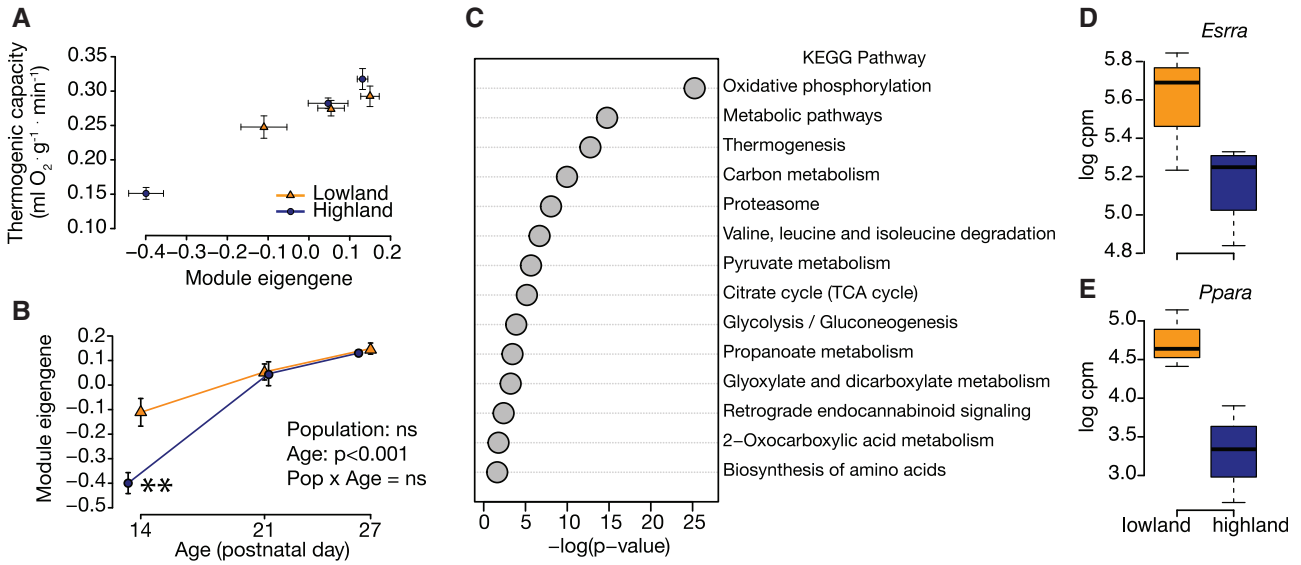

FIG. 4. Skeletal muscle module M6 is significantly associated with thermogenic capacity in lowland (orange, triangles) and highland (blue, circles) deer mice aged p14–p27. (*A*) Module expression is positively correlated with thermogenic capacity at the population/age level (individual-level data not available). (*B*) Highland deer mice exhibit significantly lower module eigengene values at postnatal day p14 (**$P < 0.01$), and no differences in expression at p21 or p27. (*C*) Functional enrichment analysis reveals enrichment of KEGG pathways involved in aerobic metabolism and thermogenesis among others (see also supplementary table S4, Supplementary Material online). Values are the negative log of the enrichment test *P* value after correction for multiple testing using the g:SCS algorithm in *gProfilerR* (Reimand et al. 2016). Expression values (log counts per million; cpm) for the transcription factors *Esrra* (*D*) and *Ppara* (*E*) at p14 are lower for highlanders compared with lowlanders; both transcription factors are involved in the regulation of mitochondrial biogenesis and metabolic pathways.

vessel development that eventually leads to a greater production of capillaries in highlanders by p21 (Robertson and McClelland 2019). Indeed, along with a greater proportion of oxidative fiber types, increased capillary density is thought to be an adaptive advantage at high altitude that contributes to improved aerobic performance capabilities in adult mice (Lui et al. 2015; Scott et al. 2015; Nikel et al. 2018).

By contrast to M2, module M6 was enriched for functions related to energy metabolism, generation of ATP, and thermogenesis, including the KEGG terms "oxidative phosphorylation, thermogenesis, citrate cycle, and glycolysis/gluconeogenesis" (fig. 4*C*). Enrichment of the GO Cellular Component terms "NADH dehydrogenase complex and mitochondrial respiratory chain complex I" indicates that energy metabolism functions are related to changes in the production of NADH: ubiquinone oxidoreductase/mitochondrial complex I, the first protein complex in the electron transport chain. We also detected significant enrichment of transcription factor binding sites for estrogen-related receptor alpha, ERR1 (supplementary table S4, Supplementary Material online; *Esrra* in the *Peromyscus* genome), which is a major regulator of mitochondrial biogenesis, gluconeogenesis, and oxidative phosphorylation. Indeed, the *Esrra* gene itself was assigned to module M6 and its expression at p14 is strongly downregulated in highlanders relative to lowlanders (fig. 4*D*). Detection of *Ppara* (peroxisome proliferator activated receptor alpha) in module M6 (fig. 4*E*) suggests that fatty acid oxidation

may also be depressed in highlanders, since this gene is a major regulator of fat metabolism in muscle (Issemann and Green 1990).

Evidence of Selection on Candidate Transcriptional Modules

Among transcriptional modules identified by WGCNA, three (B3, B36, and M6) were significantly and positively associated with variation in VO_2. These modules represent candidate pathways underlying the delay in thermogenesis in high-altitude mice. We took a two-pronged approach to determine whether developmental delays in candidate module expression are adaptive at high altitude. First, we calculated P_{ST} (an estimate of phenotypic differentiation following Brommer [2011]) on module eigengene values of candidate modules to test whether divergence between lowland and highland populations exceeds the expectation set by neutral genetic differentiation (F_{ST}; estimated with Weir's Theta; Weir and Cockerham 1984). P_{ST} was calculated across a range of c/h^2 values from 0 (no heritability) to 2, which is where the relationship between c/h^2 and P_{ST} reaches asymptote (Brommer 2011; fig. 5); the ratio c/h^2 represents the degree to which phenotypic differences are due to additive genetic effects and cannot be readily estimated using our data. For candidate BAT modules B3 and B36, P_{ST} was significantly greater ($\alpha = 0.05$) than F_{ST} above extremely conservative estimates of c/h^2 that approached zero (B3: $c/h^2 < 0.11$; B36: $c/h^2 < 0.08$; fig. 5A and B). Using 99% confidence intervals raised the value of c/h^2 for which P_{ST} significantly exceeds F_{ST}, though this value remained at extremely conservative levels (B3: $c/h^2 < 0.14$; B36: $c/h^2 < 0.15$). We note that in all cases the values of c/h^2 for which P_{ST} is greater than F_{ST} are far lower than Brommer's (2011) null expectation of $c/h^2 = 1$, suggesting that phenotypic differences are very unlikely to be caused by drift alone. This interpretation is further supported by the critical c/h^2, which for B3 and B36 are extremely low (<0.13; supplementary table S5, Supplementary Material online). By contrast to B3 and B36, confidence intervals for P_{ST} calculated on B0 (not associated with thermogenesis) overlap entirely with F_{ST} at all values of c/h^2 (fig. 5C), indicating that differentiation in expression of this module is nonsignificant and does not exceed neutral expectations. P_{ST} calculated on VO_2 across p0–p10 did not exceed the upper 95% limit of F_{ST}, except when we restricted it to p10 (supplementary fig. 2, Supplementary Material online), the time point under which cold-induced VO_2 is significantly lower in highlanders compared with lowlanders (fig. 1A).

We found that P_{ST} on the skeletal muscle module M6 did not exceed neutral expectations: although observed mean P_{ST} does exceed the upper 95% limit of F_{ST}, 95% confidence limits for both values overlap entirely with zero (supplementary fig. S1, Supplementary Material online). We note that P_{ST} does not tend to overlap with the upper 95% limit of F_{ST} when we restrict it to p14 (the time point of significant differentiation in module expression and thermogenic capacity; figs. 1B and 4B; see supplementary fig. S2, Supplementary Material online). This pattern of phenotypic differentiation is mirrored by P_{ST} on thermogenic capacity at p14, which greatly exceeds the upper 95% limit of F_{ST} at all values of c/h^2 (supplementary fig. S2, Supplementary Material online).

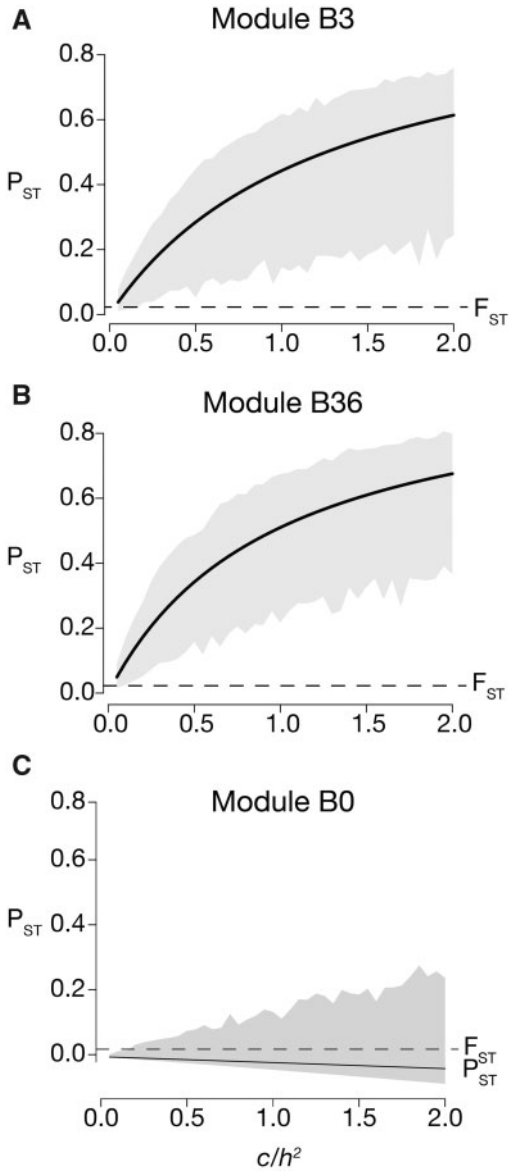

FIG. 5. P_{ST} on module eigengene values for BAT modules B3 (A), B36 (B), and B0 (C), which constitutes a suite of uncorrelated genes. P_{ST} values were calculated across a range of unknown c/h^2 values from 0 to 2. Gray polygons represent 95% confidence limits on P_{ST}. The upper 95% confidence of F_{ST} are shown as a dashed line. Ninety-five percent confidence intervals for both values were generated by bootstrapping. Nonoverlap between the lower limit of P_{ST} and upper F_{ST} confidence limits indicates a significant difference at $\alpha = 0.05$. For nearly every value of P_{ST} for modules B3 and B36, but not B0, P_{ST} is significantly greater than F_{ST}.

Finally, we tested whether these candidate VO_2-associated transcriptional modules were enriched for genes exhibiting signatures of positive natural selection, as measured by the population branch statistic (PBS; Yi et al. 2010). Roughly 25% of the genes in modules B3, B36, and M6 contained single-nucleotide polymorphisms (SNPs) with PBS values that exceeded neutral expectations (table 3). However, only B36

Table 3. Number and Proportion of Genes in Candidate Modules Containing Outlier SNPs (PBS > 99.9% quantile of the simulated distribution).

Module	No. Outlier Genes	Total Genes	% Outlier Genes	*P* Value
B3	**184**	**773**	**23.8**	**0.7**
B36	**196**	**708**	**27.7**	***0.02***
M6	**631**	**2,878**	**21.9**	**1**

NOTE.—*P* values obtained from Fisher's exact tests. Significant *P*-values are italicized.

exhibited a significant enrichment of outlier SNPs relative to the background rate (Fisher's exact test, $P = 0.02$; table 3). This analysis demonstrates that, although all phenotype-associated modules exhibit some proportion of genes under selection, only B36 contains more than was expected by chance.

Discussion

We explored the mechanisms that underlie a developmental delay in the onset of thermogenesis in juvenile high-altitude deer mice (fig. 1). We show that the developmental trajectory of the thermoregulatory system has evolved at high altitude *via* selection on the regulatory systems that control the development of thermoeffector tissues, BAT and skeletal muscle. Combined with the results of Robertson et al. (2019) and Robertson and McClelland (2019), our work suggests that the cold hypoxic conditions of high altitude force an alternative resource allocation strategy, whereby limited energy is put into developmental processes such as growth, over the development of the thermoregulatory machinery needed in heat production.

A Developmental Delay in NST Is Associated with a Delay in Expression of Fuel Supply, Oxygenation, and Axon Guidance Pathways in BAT

During early postnatal development mice rely exclusively on BAT for thermogenesis, and low-altitude pups activate BAT to maintain body temperature in the face of cold by p10. Our analysis suggests that an ontogenetic delay in the development of NST in high-altitude deer mice (fig. 1A) is attributable to a delay in the nervous system innervation and O_2/fuel supply lines to a maturing BAT. WGCNA of BAT revealed two transcriptional modules (B3, B36) that are expressed at higher levels in lowlanders across age (fig. 3). Both modules were correlated with cold-induced VO_2, suggesting that changes in the expression of genes in these modules influence the development of thermogenesis. Module B3 was enriched for pathways involved in metabolism, particularly fatty acid degradation (fig. 3 and supplementary table S4, Supplementary Material online). This is compelling since fat is the primary fuel source that powers uncoupling of cellular respiration from ATP production in nonshivering heat production (Cannon and Nedergaard 2004). Indeed, the β3 signaling cascade, initiated by cold, stimulates the lipolysis of fats used in β-oxidation and the eventual uncoupling of ATP synthesis from electron transport *via* activation of Uncoupling Protein 1 (*Ucp1*). Although not assigned to B3, we found that expression of *Ucp1* itself was lower in highlanders compared with lowlanders (analysis of variance [ANOVA], main effect of population; $F_{1,30} = 8.2$; $P = 0.007$).

Module B36, by contrast, was enriched for two pathways that are important in O_2/fuel supply and cold-activation of BAT. For example, enrichment of the VEGF signaling pathway, and downregulation of *Vegfa* in highlanders (fig. 3B), suggests a reduction in the vascularization of BAT early in the postnatal period in high-altitude natives. This is notable since the VEGF cascade stimulates angiogenesis, increasing O_2 and metabolic fuel delivery. Moreover, *Vegfa* itself contains two SNPs above the 99.9% PBS threshold (Schweizer, Velotta et al. 2019), suggesting that changes in the VEGF pathway are one of many targets of selection at high altitude. We also detected enrichment of the KEGG pathway "axon guidance," which represents a key stage in development in which neurons send out axons to reach their targets. Indeed, BAT is activated by the sympathetic nervous system in response to cold, which leads to the release of norepinephrine and the signaling cascade that produces heat (Cannon and Nedergaard 2004).

A reduction in the expression of genes that participate in axon guidance suggests a developmental delay in the sympathetic innervation of BAT, which would inhibit recruitment and activation of this tissue during cold exposure (Robertson et al. 2019). Robertson et al. (2019) found lower levels of the enzyme tyrosine hydroxylase in the BAT of high-altitude pups at p10, lending support to the hypothesis that neurotransmitter synthesis and neural activation of BAT tissue is delayed in highlanders; tyrosine hydroxylase is the rate-limiting enzyme in norepinephrine production and is present in sympathetic neurons innervating BAT. Related to the reduced sympathetic activation of BAT, we found that expression of the gene *calsyntenin 3* (*Clstn3*) is also downregulated in highlanders (ANOVA, main effect of population; $F_{1,30} = 15.1$; $P < 0.001$). *Clstn3* is a known promoter of synapse formation; a recent study in house mice found that a mammalian-specific form (*Clstn3*β) enhances functional sympathetic innervation of BAT (Zeng et al. 2019).

Despite downregulation of genes involved in O_2/fuel supply and innervation of BAT, Robertson et al. (2019) found that BAT mass does not differ between highlanders and lowlanders, and that citrate synthase (a biomarker of mitochondrial abundance) and UCP protein expression are likewise equivalent. Our results therefore suggest that, although BAT growth and metabolic potential may be equal in highlanders and lowlanders, a delay in the development of the innervation and O_2/fuel supply to BAT may lead to an inability of highlanders to respond to cold temperatures and thus mount an appropriate thermoregulatory response.

A Developmental Delay in Thermogenic Capacity Is Associated with Downregulation of Energy Metabolism Pathways in Muscle

Transcriptome analysis of skeletal muscle revealed a large transcriptional module (M6) that closely tracked variation in thermogenic capacity (fig. 4). This result suggests that

the genes expressed in module M6 underlies the developmental delay in thermogenesis beyond p10 (fig. 1B). The M6 module (table 2) was enriched for a host of functions related to skeletal muscle metabolism that reflect changes in its maturation with respect to shivering. Our analysis suggests that high-altitude mice show a developmental delay in the expression of nearly all pathways related to ATP generation by mitochondria, including glycolysis, citrate cycle, and oxidative phosphorylation (fig. 4C). Many of the genes that contribute to functional enrichment of metabolic pathways were related to the production of mitochondrial respiratory complex I, including 31 of 35 *Nduf* genes, suggesting that downregulation of metabolic pathways may be related to a delay in mitochondrial biogenesis. Indeed, the GO terms "mitochondria and mitochondrial part" were also enriched (supplementary table S4, Supplementary Material online).

At least two transcription factors that are key regulators of cellular metabolism were found in module M6 and were expressed at lower levels in highlanders (fig. 4D and E). Estrogen-related receptor alpha, *Esrra*, for example, directs the expression of genes involved in mitochondrial biogenesis (Wu et al. 1999) and mitochondrial energy-producing pathways in skeletal muscle (Huss et al. 2004). Genes in module M6 were also enriched for *Esrra* binding sites (supplementary table S4, Supplementary Material online). Lowered expression of peroxisome proliferator activated receptor alpha (*Ppara*) suggests that fatty acid oxidation may also be depressed in highlanders, since this gene is a major regulator of fat metabolism capacity; functional terms related to fat oxidation however were not enriched in this module (supplementary table S4, Supplementary Material online). Indeed, Robertson and McClelland (2019) found that the β-oxidation enzyme β-hydroxyacyl-CoA dehydrogenase did not track changes in muscle aerobic capacity of highlanders over these ages. These data provide evidence that the developmental delay in thermogenic capacity is linked to a delay in the expression of pathways that facilitate mitochondrial development and muscle aerobic capacity and allow for shivering thermogenesis.

Evidence of Natural Selection

We found that population divergence in expression of VO_2-associated transcriptional modules exceeded neutral expectations set by genetic differentiation (measured as F_{ST}), suggesting that population differences may be adaptive. We expected that, if population divergence in module expression was adaptive, P_{ST} on module eigengene would exceed the upper bounds of the confidence intervals around our estimate of F_{ST}. At extremely low and conservative values of c/h^2 (i.e., $c/h^2 < 1$, the null expectation according to Brommer [2011]), the lower confidence limits of P_{ST} for candidate BAT modules B3 and B36 exceeded the upper confidence limits of F_{ST} (fig. 5A and B), indicating significant differences. These results hold true when 95% and 99% confidence intervals are used, suggesting that population-level expression differences in candidate BAT modules are highly unlikely to be caused by drift alone. This finding is consistent with P_{ST} on cold-induced VO_2 values at p10 (supplementary fig. S2, Supplementary Material online), the time point of greatest population differentiation (fig. 1A). Although P_{ST} did not exceed F_{ST} for the skeletal muscle module M6 across all time points (p14–p27), we did find it to exceed neutral expectations when restricted to p14 (supplementary fig. S2, Supplementary Material online). This is consistent with the finding that P_{ST} on thermogenic capacity also exceeds the upper 95% of F_{ST} at p14 only (supplementary fig. S2, Supplementary Material online). Together these data suggest that the delay in the onset of NST and shivering thermogenesis, and their underlying regulatory control pathways, may be the target of selection at high altitude.

Approximately 25% of genes in candidate modules bear the signature of natural selection, that is, they contain at least one SNP above the PBS significance threshold (table 3). Only module B36, however, was significantly enriched for PBS outliers above the transcriptome-wide background level. Such sequence divergence within candidate module genes may be the result of selection at the *cis*-regulatory regions that modulate individual gene expression. However, that we do not detect a higher proportion of candidate module genes bearing the signature of natural selection is not unexpected, as selection on upstream *trans*-regulatory elements may influence the expression of many genes in a single network. We note that it is not possible to discern with certainty whether the genetic variants we identified are the direct targets of selection, as these loci may be linked to casual variants. Pinpointing the genetic variants that influence candidate pathway expression and the delay in the development of thermogenesis will be the focus of future work. Nevertheless, because PBS is polarized by the use of a second lowland population (see Materials and Methods), we can discern that the outlier loci we do detect (or closely linked loci) are under positive selection in the high-altitude population. Our results support the interpretation that differentiation in expression of candidate modules, at least within BAT, is driven, in part, by natural selection.

Summary and Conclusions

We found that a developmental delay in the onset of independent thermoregulatory ability in deer mice native to high altitude is rooted in a delay in the expression of gene regulatory networks that contribute to sympathetic innervation of BAT that permits the response to cold, and in pathways that contribute to fuel use and ATP production of both thermoeffector organs. Phenotypic divergence analysis suggests that both thermogenic delays and associated shifts in gene expression in BAT are driven by natural selection. An overabundance of genes exhibiting signatures of natural selection in BAT module B36 suggests that developmental changes to genes in this module may be particularly important in high-altitude adaptation. Our results demonstrate that changes to the developmental trajectory of thermoregulation at high altitude are the result of regulatory delays in the development of thermoeffector organs, which limit the ability of high-altitude mice to mount a thermoregulatory response.

Our results support the hypothesis that the developmental delay in thermogenesis at high altitude is attributable to an

adaptive energetic tradeoff (Robertson et al. 2019; Robertson and McClelland 2019). The observed developmental delay in expression of transcriptional pathways associated with neural activation and energy production suggests that the BAT and skeletal muscles of high-altitude mice take longer to fully mature postnatally, relative to lowlanders. That growth rate is equivalent between high- and low-altitude pups under common conditions (Robertson et al. 2019) suggests that high-altitude mice may allocate energy toward growth instead of into the maturation of thermoeffector tissues that promote active thermogeneration. The combination of chronic cold and low O_2 availability at high altitude, coupled with larger litter sizes that should affect competition among siblings for limited resources (Robertson et al. 2019), may contribute to the altered energetic conditions that drive this tradeoff. Because high-altitude adult deer mice show the opposite pattern compared with developing pups (i.e., consistently higher thermogenic capacities, Cheviron et al. 2013), we suggest that selection pressures at high altitude can have very different effects on the same physiological systems, depending on age. Future work on the selective drivers and energetic benefits of this putatively adaptive energy allocation strategy will shed light on adaptive modification of developmental processes to meet the challenge of selection pressures that vary in strength and magnitude across ontogeny.

Materials and Methods

Animals and Experimental Procedures

Deer mice used in this study were F_2 lab-reared descendants of two wild populations of *Peromyscus maniculatus* (Robertson et al. 2019; Robertson and McClelland 2019) raised under common environmental conditions (24 °C, 80 m a.s.l.) at McMaster University of Ontario, Canada. Individuals from the high-altitude population were captured from the summit of Mount Evans in Clear Creek County, CO, USA (4,350 m a.s.l.) and the low-altitude population from Nine-mile prairie, NE, USA (320 m a.s.l.). F_2 pups were derived from one of the first three litters produced by their F_1 parental breeding pair (family). A total of 7 lowland and 11 highland families were used. At each developmental age, two individuals from each family (one male and one female, when possible) were sampled. Sampling time points were randomly distributed across the three litters.

Altricial rodents, such as deer mice, usually develop NST prior to shivering due to the maturation of BAT which precedes the maturation of skeletal muscle. *P. maniculatus* are only capable of NST after the first 10 days postpartum (Robertson et al. 2019). In contrast, shivering develops between 2 and 4 weeks after birth (Robertson and McClelland 2019). We sampled BAT and skeletal muscle (specifically, the gastrocnemius) over these two periods. Briefly, pups were removed from the nest, then euthanized with an overdose of isoflurane followed by cervical dislocation. In pups ages 0, 2, 4, 6, 8, and 10 days postpartum the intrascapular depot of BAT was blunt dissected and cleaned of white adipose tissue. In pups aged 14, 21, and 27 days postpartum the gastrocnemius muscle of the lower hindlimb was blunt dissected. Tissues were flash frozen and stored at −80 °C.

We reanalyzed cold-induced O_2 consumption rate (VO_2) data from Robertson et al. (2019) and Robertson and McClelland (2019) for low- and high-altitude native *P. maniculatus* only, omitting the low-altitude congeneric, *Peromyscus leucopus*. Briefly, for pups aged 0–10 days postpartum cold-induced VO_2 was assessed in response to a mild cold stress (10 min at 24 °C). Pups were compared with a control litter mate who was maintained at 30 °C for the same duration of trial in order to control for handling stress. For pups aged 14–27 days, maximum cold-induced VO_2 (thermogenic capacity) was measured using previously established methods for adult deer mice (Cheviron et al. 2012). VO_2max was induced by exposing pups to −5 °C in heliox air (21% O_2 with He). All VO_2 measurements were divided by mass to obtain mass-specific metabolic rates.

Transcriptome Analyses

We conducted high-throughput sequencing of RNA of BAT and skeletal muscle in order to explore the mechanisms that underlie developmental delays in thermogenesis. Sample size varied from $n = 1$–7 for each population, age, and tissue (see supplementary table S1, Supplementary Material online, in online supplementary material for full list). We assayed gene expression using TagSeq, a 3′ tag-based sequencing method following Lohman et al. (2016). First, we extracted RNA from <25 mg of tissue using TRI Reagent (Sigma-Aldrich), then assessed RNA quality using TapeStation (Agilent Technologies; RNA Integrity Number > 7). The Genome Sequencing and Analysis Facility at the University of Texas at Austin prepared TagSeq libraries, which were sequenced using Illumina HiSeq 2500. We filtered raw reads for length, quality, and polymerase chain reaction duplicates following Lohman et al. (2016) using scripts modified from those available online (https://github.com/z0on/tag-based_RNAseq; last accessed April 16, 2020). Using the FASTX-toolkit (http://hannonlab.cshl.edu/fastx_toolkit/; last accessed April 16, 2020), we cleaned and trimmed raw reads, which resulted in 3.2 million reads per individual. Filtered reads were then mapped to the *P. maniculatus* genome (NCBI GCA_000500345.1 Pman_1.0) using *bwa mem* (Li and Durbin 2010). Across all samples, ∼64–79% of raw reads mapped to the *P. maniculatus* genome. We detected 3% lowered mapping success, on average, in lowland individuals in the BAT transcriptome (linear mixed effects model; $F_{1,8.2} = 5.6$; $P = 0.04$), but no population difference in the skeletal muscle transcriptome ($P > 0.05$). We used *featureCounts* (Liao et al. 2014) to generate a table of transcript abundances. Since genes with low read counts are subject to measurement error (Robinson and Smyth 2007), we excluded those with less than an average of 10 reads per individual. We retained a total of 11,192 and 11,104 genes after filtering for BAT and skeletal muscle transcriptomes, respectively. Five outlier samples (one BAT, four skeletal muscle) were removed following visual inspection of multidimensional scaling plots using *plotMDS* in *edgeR* following Chen et al. (2019).

We assessed overall patterns of gene expression among BAT and skeletal muscle transcripts using PCA, whereas WGCNA (v. 1.41-1; Langfelder and Horvath 2008) was used to identify potential regulatory mechanisms that underlie variation in thermogenesis across development. PCA and WGCNA analyses were conducted separately on BAT and skeletal muscle samples in R v. 2.5.2 (R Core Team). WGCNA identified clusters of genes with highly correlated expression profiles (modules). This approach was successfully implemented in recent studies that aimed to relate gene expression with higher-level phenotypes (Plachetzki et al. 2014; Velotta et al. 2016, 2018). Prior to performing WGCNA, we normalized raw read counts by library size and log-transformed them using the functions *calcNormFactors* and *cpm*, respectively, from the R package *edgeR* (Robinson et al. 2010). Module detection was performed using the *blockwiseModules* function in WGCNA with *networkType* set to "signed" (Langfelder and Horvath 2008). Briefly, Pearson correlations of transcript abundance data were calculated between pairs of genes, after which an adjacency matrix was computed by raising the correlation matrix to a soft thresholding power of $\beta = 6$. Soft thresholding power β is chosen to achieve an approximately scale free topology, an approach that favors strong correlations (Zhang and Horvath 2005). We chose a $\beta = 6$ since it represents the value for which improvement of scale free topology model fit begins to decrease with increasing thresholding power. A topological overlap measure was computed from the resulting adjacency matrix for each gene pair. Topologically based dissimilarity was then calculated and used as input for average linkage hierarchical clustering in the creation of cluster dendrograms for both tissues. Modules were identified as branches of the resulting cluster tree using the dynamic tree-cutting method (Langfelder and Horvath 2008). We assigned modules a unique identification according to tissue (B0–B37 for BAT; M0–M7 for skeletal muscle). Genes that could not be clustered into a module were given the designation B0 and M0 for BAT and skeletal muscle, respectively.

Once modules were defined, we used a multistep process to associate expression among individuals with variation in VO_2. First, we summarized module expression using PCA of gene expression profiles (*blockwiseModules* in WGCNA); because genes within modules are highly correlated by definition, the first principal component axis (referred to as the module eigengene) was used to represent module expression (Langfelder and Horvath 2008). We used module eigengene values to test for associations between module expression and VO_2 for each module (Pearson correlation; *cor* function in WGCNA) in the BAT network. *P* values for the correlation were determined by a Student's asymptotic test (*corPvalueStudent* in WGCNA). For skeletal muscle, association tests were conducted on population-age means since VO_2 measurements do not exist for the individuals sequenced. Among phenotype-associated modules, we conducted analysis-of-variance (ANOVA) on rank-transformed module eigengene values in order to test for the effects of population, age, and their interaction on module expression. *P* values from association tests and ANOVAs were corrected for multiple testing using the false-discovery rate method (Benjamini and Hochberg 1995).

We performed functional enrichment analysis on all modules exhibiting either a statistical association with VO_2, or a significant effect in ANOVA, or both, using the R package *gProfilerR* (Reimand et al. 2016). *P. maniculatus* gene names were converted to *Mus musculus* gene names (Online supplementary material) using a custom script. We corrected for multiple testing using *gProfilerR's* native g: SCS algorithm. We used the list of genes from filtered BAT and skeletal muscles transcriptomes as a custom background list in all enrichment analyses. We searched for enrichment among terms from GO (Ashburner et al. 2000; Gene Ontology Consortium 2019), KEGG (Kanehisa and Goto 2000), Reactome (Fabregat et al. 2018), and WikiPathways (Slenter et al. 2018) databases, as well as transcription factor binding sites from the TRANSFAC database (Matys et al. 2006).

Tests of Phenotypic and Genetic Divergence

We used two complementary approaches to assess phenotypic and genetic divergence to test for signatures of natural selection in VO_2-associated modules. To assess phenotypic divergence, we calculated P_{ST} on module eigengene values following Brommer (2011) using equation (1):

$$P_{ST} = \frac{\frac{c}{h^2}\sigma_B^2}{\frac{c}{h^2}\sigma_B^2 + 2\sigma_W^2}, \quad (1)$$

where σ_B^2 denotes between-population phenotypic variance, σ_W^2 denotes within-population phenotypic variance, h^2 the narrow-sense heritability (the proportion of phenotypic variance that is due to additive genetic effects), and c a scalar representing the total phenotypic variance due to additive genetic effects across populations. Within- and between-population variances were estimated from ANOVA, where module eigengene values were response variables, and post-natal day, population, and family nested within population were included as main effects. Within-population variance (σ_W^2) was calculated as the residual mean squares (MS) from the ANOVA model. Between-population variance was estimated after Antoniazza et al. (2010) following equation (2):

$$\sigma_B^2 = \frac{MS_B - MS_W}{n_0}, \quad (2)$$

where MS_B and MS_W are the population effect and the residual mean square variances from the ANOVA model, respectively, and n_0 a weighted average of sample size based on Sokal and Rohlf (1995) following equation (3):

$$n_0 = \frac{(n_1 + n_2) - (n1^2 + n_2{}^2)}{n_1 + n_2}, \quad (3)$$

where n_1 and n_2 are the sample sizes of population one and two, respectively. The ratio c/h^2 was unknown and could not be estimated using our experimental design. As such, we calculated P_{ST} across a range of values of c/h^2 from 0 (no heritability) to 2, which is where the relationship between

c/h^2 and P_{ST} begins to reach asymptote (Brommer 2011; fig. 5). We calculated 95% and 99% confidence intervals for each value of P_{ST} calculated across values of c/h^2 ranging from 0 to 2 at 0.05 level increments (total of 40 P_{ST} estimates). Confidence intervals for each P_{ST} value were estimated with bootstrapping (with 1,000 replicates) using the *boot* function in R.

P_{ST} estimates were compared with neutral divergence expectations set by between-population differentiation. We calculated pairwise genetic differentiation between the lowland and highland populations using F_{ST} (estimated with Weir's Theta; Weir and Cockerham 1984) and previously sequenced exome data (Schweizer, Velotta et al. 2019). Briefly, F_{ST} was calculated for 5,183,435 high-quality biallelic SNPs using the "–weir-fst-pop" flag within vcftools v0.1.16 (Danecek et al. 2011). We pruned SNPs for linkage-disequilibrium using the "indep-pairwise 50 5 0.5" flag in PLINK1.9 (Chang et al. 2015) and restricted the data to non-genic, putatively neutral, regions of the exome (Schweizer, Velotta et al. 2019), leading to a reduced set of 172,408 SNPs. We then calculated 95% and 99% confidence intervals around the estimate of mean F_{ST} (0.022) with bootstrapping by randomly sampling a subset of 10,000 SNPs, with replacement, 10,000 times (*boot* function in R). Significant differences between P_{ST} and F_{ST} were determined by nonoverlap between the upper confidence limits of F_{ST} and lower limits of P_{ST} for $\alpha = 0.05$ for 95% confidence limits, and $\alpha = 0.01$ for 99% confidence limits. Finally, we calculated the critical c/h^2 value following Brommer (2011), which represents the ratio at which confidence intervals around P_{ST} equal the confidence interval around F_{ST}. These results are presented in supplementary table S5, Supplementary Material online, for ease of comparison to other published quantitative analyses.

We then compared P_{ST} of each candidate VO_2-associated module with that of "module 0," which contains the suite of genes that could not be reliably clustered (B0 in BAT; M0 in skeletal muscle). The null expectation is that P_{ST} should not exceed the neutral expectation set by F_{ST} at any value of c/h^2. We expected that, if natural selection has shaped shifts in gene expression, then P_{ST} would exceed F_{ST} in VO_2-associated modules, but not in modules B0 or M0 (which serve as a measure of background levels of expression differentiation). We calculated P_{ST} on cold-induced VO_2 (p0–p10) and thermogenic capacity (p14–p27) as above in order to determine whether these higher-level phenotypic traits were also the targets of natural selection.

Finally, we took a population genomic approach to assess whether genes in VO_2-associated transcriptional modules exhibit signatures of positive natural selection at high altitude. To do this, we used PBS (Yi et al. 2010) data from Schweizer, Velotta et al. (2019). Here, PBS identifies loci that exhibit extreme allele frequency differences in highland (Mt Evans) relative to lowland (Lincoln and Merced, CA) populations. We previously calculated PBS for 5,183,435 exome-wide biallelic SNPs, then calculated the demographically corrected significance of PBS values using a simulated distribution of 500,000 SNPs (see Schweizer, Velotta et al. 2019 for simulation details). We first determined significant outlier SNPs with a PBS value located above the 99.9% quantile, then identified those SNPs located within genes belonging to VO_2-associated modules using Ensembl's Variant Effect Predictor (McLaren et al. 2010) with the *P. maniculatus* reference genome annotation data set. We used Fisher's exact tests to determine whether thermogenesis-associated modules were statistically enriched for loci that exceeded the 99.9% threshold.

Supplementary Material

Supplementary data are available at *Molecular Biology and Evolution* online.

Acknowledgments

We thank Maria Stager and Timothy Moore for help with statistical analyses. We also thank Kamilla Bentsen and Madilyn Head for help extracting RNA. This study was funded by the National Institutes of Health, National Heart, Lung, and Blood Institute, Research Service Award Fellowship (1F32HL136124-01 to J.P.V.); the National Science Foundation (Postdoctoral Research Fellowship in Biology 1612859 to R.M.S. and IOS-1755411 and OIA 1736249 to Z.A.C.); the National Sciences and Engineering Research Council of Canada Discovery (Grant No. RGPIN 462246-2014) and a Canada Graduate Scholarship to G.B.M. and C.E.R.

References

Antoniazza S, Burri R, Fumagalli L, Goudet J, Roulin A. 2010. Local adaptation maintains clinal variation in melanin-based coloration of European barn owls (*Tyto alba*). *Evolution* 64:1944–1954.

Arjamaa O, Lagerspetz K. 1979. Postnatal development of shivering in the mouse. *J Therm Biol*. 4(1):35–39.

Ashburner M, Ball CA, Blake JA, Botstein D, Butler H, Cherry JM, Davis AP, Dolinski K, Dwight SS, Eppig JT, et al. 2000. Gene Ontology: tool for the unification of biology. Nat Genet. 25(1):25–29.

Beall CM. 2007. Two routes to functional adaptation: Tibetan and Andean high-altitude natives. *Pro Natl Acad Sci U S A*. 104(Suppl 1):8655–8660.

Benjamini Y, Hochberg Y. 1995. Controlling the false discovery rate: a practical and powerful approach to multiple testing. *J R Stat Soc Ser B Methodol*. 57(1):289–300.

Bouverot P. 1985. Adaptation to altitude-hypoxia in vertebrates. Berlin: Springer Science & Business Media.

Brommer JE. 2011. Whither Pst? The approximation of Qst by Pst in evolutionary and conservation biology. *J Evol Biol*. 24(6):1160–1168.

Campbell-Staton SC, Bare A, Losos JB, Edwards SV, Cheviron ZA. 2018. Physiological and regulatory underpinnings of geographic variation in reptilian cold tolerance across a latitudinal cline. *Mol Ecol*. 27(9):2243–2255.

Campbell-Staton SC, Cheviron ZA, Rochette N, Catchen J, Losos JB, Edwards SV. 2017. Winter storms drive rapid phenotypic, regulatory, and genomic shifts in the green anole lizard. *Science* 357(6350):495–498.

Cannon B, Nedergaard J. 2004. Brown adipose tissue: function and physiological significance. *Physiol Rev*. 84(1):277–359.

Chang CC, Chow CC, Tellier LC, Vattikuti S, Purcell SM, Lee JJ. 2015. Second-generation PLINK: rising to the challenge of larger and richer datasets. *GigaScience* 4(1):7.

Chappell MA, Snyder LR. 1984. Biochemical and physiological correlates of deer mouse alpha-chain hemoglobin polymorphisms. *Proc Natl Acad Sci U S A*. 81(17):5484–5488.

Chen Y, McCarthy DJ, Ritchie M, Robinson M, Smyth GK. 2019. edgeR: differential expression analysis of digital gene expression data User's

Guide. Available from: http://scholar.googleusercontent.com/scholar?q=cache:wKdKwEukm7wJ:scholar.google.com/+edgeR+and+outlier&hl=en&as_sdt=0,27. Accessed April 16, 2020.
Cheviron ZA, Bachman GC, Connaty AD, McClelland GB, Storz JF. 2012. Regulatory changes contribute to the adaptive enhancement of thermogenic capacity in high-altitude deer mice. *Proc Natl Acad Sci U S A*. 109(22):8635–8640.
Cheviron ZA, Bachman GC, Storz JF. 2013. Contributions of phenotypic plasticity to differences in thermogenic performance between highland and lowland deer mice. *J Exp Biol*. 216(7):1160–1166.
Cheviron ZA, Connaty AD, McClelland GB, Storz JF. 2014. Functional genomics of adaptation to hypoxic cold-stress in high-altitude deer mice: transcriptomic plasticity and thermogenic performance. *Evolution* 68(1):48–62.
Danecek P, Auton A, Abecasis G, Albers CA, Banks E, DePristo MA, Handsaker RE, Lunter G, Marth GT, Sherry ST, et al. 2011. The variant call format and VCFtools. *Bioinformatics* 27(15):2156–2158.
DeBiasse MB, Kelly MW. 2016. Plastic and evolved responses to global change: what can we learn from comparative transcriptomics? *J Hered*. 107(1):71–81.
Fabregat A, Jupe S, Matthews L, Sidiropoulos K, Gillespie M, Garapati P, Haw R, Jassal B, Korninger F, May B, et al. 2018. The reactome pathway knowledgebase. *Nucleic Acids Res*. 46(D1):D649–D655.
Garland T, Carter PA. 1994. Evolutionary physiology. *Annu Rev Physiol*. 56(1):579–621.
Garland T, Losos JB. 1994. Ecological morphology of locomotor performance in squamate reptiles. In: Wainwright PC, Reilly SM, editors. Ecological morphology: integrated organismal biology. Chicago (IL): Chicago University Press. p. 240–302.
Hayes JP, O'Connor CS. 1999. Natural selection on thermogenic capacity of high-altitude deer mice. *Evolution* 53(4):1280–1287.
Hill RW. 1983. Thermal physiology and energetics of *Peromyscus*; ontogeny, body temperature, metabolism, insulation, and microclimatology. *J Mammal*. 64(1):19–37.
Huey RB, Stevenson RD. 1979. Integrating thermal physiology and ecology of cctotherms: a discussion of approaches. *Am Zool*. 19(1):357–366.
Huss JM, Torra IP, Staels B, Giguère V, Kelly DP. 2004. Estrogen-related receptor α directs peroxisome proliferator-activated receptor α signaling in the transcriptional control of energy metabolism in cardiac and skeletal muscle. *Mol Cell Biol*. 24(20):9079–9091.
Irschick DJ, Garland T. 2001. Integrating function and ecology in studies of adaptation: investigations of locomotor capacity as a model system. *Annu Rev Ecol Syst*. 32(1):367–396.
Irschick DJ, Meyers JJ, Husak JF, Galliard J-F. 2008. How does selection operate on whole-organism functional performance capacities? A review and synthesis. *Evol Ecol Res*. 10:177–197.
Issemann I, Green S. 1990. Activation of a member of the steroid hormone receptor superfamily by peroxisome proliferators. *Nature* 347(6294):645–650.
Ivy CM, Scott GR. 2017. Control of breathing and ventilatory acclimatization to hypoxia in deer mice native to high altitudes. *Acta Physiol*. 221(4):266–282.
Kanehisa M, Goto S. 2000. KEGG: Kyoto Encyclopedia of Genes and Genomes. *Nucleic Acids Res*. 28(1):27–30.
King JA. 1968. Biology of *Peromyscus* (*Rodentia*). Stillwater, OK: American Society of Mammologists.
Lagerspetz K. 1966. Postnatal development of thermoregulation in laboratory mice. *Helgolander Wiss Meeresunters* 14(1–4):559–571.
Lailvaux SP, Husak JF. 2014. The life history of whole-organism performance. *Q Rev Biol*. 89(4):285–318.
Langfelder P, Horvath S. 2008. WGCNA: an R package for weighted correlation network analysis. *BMC Bioinformatics* 9(1):559.
Lau DS, Connaty AD, Mahalingam S, Wall N, Cheviron ZA, Storz JF, Scott GR, McClelland GB. 2017. Acclimation to hypoxia increases carbohydrate use during exercise in high-altitude deer mice. *Am J Physiol Regul Integr Comp Physiol*. 312(3):R400–R411.
Li H, Durbin R. 2010. Fast and accurate long-read alignment with Burrows–Wheeler transform. *Bioinformatics* 26(5):589–595.
Liao Y, Smyth GK, Shi W. 2014. featureCounts: an efficient general purpose program for assigning sequence reads to genomic features. *Bioinformatics* 30(7):923–930.
Lohman BK, Weber JN, Bolnick DI. 2016. Evaluation of TagSeq, a reliable low-cost alternative for RNAseq. *Mol Ecol Resour*. 16(6):1315–1321.
Lui MA, Mahalingam S, Patel P, Connaty AD, Ivy CM, Cheviron ZA, Storz JF, McClelland GB, Scott GR. 2015. High-altitude ancestry and hypoxia acclimation have distinct effects on exercise capacity and muscle phenotype in deer mice. *Am J Physiol Regul Integr Comp Physiol*. 308(9):R779–R791.
Mahalingam S, McClelland GB, Scott GR. 2017. Evolved changes in the intracellular distribution and physiology of muscle mitochondria in high-altitude native deer mice. *J Physiol*. 595(14):4785–4801.
Matys V, Kel-Margoulis OV, Fricke E, Liebich I, Land S, Barre-Dirrie A, Reuter I, Chekmenev D, Krull M, Hornischer K. 2006. TRANSFAC® and its module TRANSCompel®: transcriptional gene regulation in eukaryotes. *Nucleic Acids Res*. 34(90001):D108–D110.
McLaren W, Pritchard B, Rios D, Chen Y, Flicek P, Cunningham F. 2010. Deriving the consequences of genomic variants with the Ensembl API and SNP Effect Predictor. *Bioinformatics* 26(16):2069–2070.
Nikel KE, Shanishchara NK, Ivy CM, Dawson NJ, Scott GR. 2018. Effects of hypoxia at different life stages on locomotory muscle phenotype in deer mice native to high altitudes. *Comp Biochem Physiol B Biochem Mol Biol*. 224:98–104.
Pembrey MS. 1895. The effect of variations in external temperature upon the output of carbonic acid and the temperature of young animals. *J Physiol*. 18(4):363–379.
Plachetzki DC, Pankey MS, Johnson BR, Ronne EJ, Kopp A, Grosberg RK. 2014. Gene co-expression modules underlying polymorphic and monomorphic zooids in the colonial hydrozoan, *Hydractinia symbiolongicarpus*. *Integr. Comp. Biol*. 54(2):276–283.
Reimand J, Arak T, Adler P, Kolberg L, Reisberg S, Peterson H, Vilo J. 2016. g: profiler—a web server for functional interpretation of gene lists (2016 update). *Nucleic Acids Res*. 44(W1):W83–W89.
Robertson CE, McClelland GB. 2019. Postnatal maturation of skeletal muscle drives adaptive thermogenic capacity of high-altitude deer mice, *Peromyscus maniculatus*. *J Exp Biol*. 222: jeb210963.
Robertson CE, Tattersall GJ, McClelland GB. 2019. Development of homeothermic endothermy is delayed in high-altitude native deer mice (*Peromyscus maniculatus*). *Proc R Soc B* 286(1907):20190841.
Robinson MD, McCarthy DJ, Smyth GK. 2010. edgeR: a Bioconductor package for differential expression analysis of digital gene expression data. *Bioinformatics* 26(1):139–140.
Robinson MD, Smyth GK. 2007. Moderated statistical tests for assessing differences in tag abundance. *Bioinformatics* 23(21):2881–2887.
Schweizer RM, Velotta JP, Ivy CM, Jones MR, Muir SM, Bradburd GS, Storz JF, Scott GR, Cheviron ZA. 2019. Physiological and genomic evidence that selection on the transcription factor *Epas1* has altered cardiovascular function in high-altitude deer mice. *PLoS Genet*. 15(11):e1008420.
Scott GR, Elogio TS, Lui MA, Storz JF, Cheviron ZA. 2015. Adaptive modifications of muscle phenotype in high-altitude deer mice are associated with evolved changes in gene regulation. *Mol Biol Evol*. 32(8):1962–1976.
Simonson TS, McClain DA, Jorde LB, Prchal JT. 2012. Genetic determinants of Tibetan high-altitude adaptation. *Hum Genet*. 131(4):527–533.
Slenter DN, Kutmon M, Hanspers K, Riutta A, Windsor J, Nunes N, Mélius J, Cirillo E, Coort SL, Digles D, et al. 2018. WikiPathways: a multifaceted pathway database bridging metabolomics to other omics research. *Nucleic Acids Res*. 46(D1):D661–D667.
Snyder L. 1981. Deer mouse hemoglobins: is there genetic adaptation to high altitude? *BioScience* 31:299–304.

Snyder LRG, Born S, Lechner AJ. 1982. Blood oxygen affinity in high- and low-altitude populations of the deer mouse. *Respir Physiol*. 48(1):89–105.
Sokal RR, Rohlf FJ. 1995. Biometry. 3rd ed. New York: W.H.H.H. Freeman and Company.
Storz JF. 2007. Hemoglobin function and physiological adaptation to hypoxia in high-altitude mammals. *J Mammal*. 88(1):24–31.
Storz JF. 2016. Hemoglobin–oxygen affinity in high-altitude vertebrates: is there evidence for an adaptive trend. *J Exp Biol*. 219(20):3190–3203.
Storz JF, Scott GR, Cheviron ZA. 2010. Phenotypic plasticity and genetic adaptation to high-altitude hypoxia in vertebrates. *J Exp Biol*. 213(24):4125–4136.
Tate KB, Ivy CM, Velotta JP, Storz JF, McClelland GB, Cheviron ZA, Scott GR. 2017. Circulatory mechanisms underlying adaptive increases in thermogenic capacity in high-altitude deer mice. *J Exp Biol*. 220(20):3616–3620.
The Gene Ontology Consortium. 2019. The Gene Ontology Resource: 20 years and still GOing strong. *Nucleic Acids Res*. 47(D1):D330–D338.
Velotta JP, Ivy CM, Wolf CJ, Scott GR, Cheviron ZA. 2018. Maladaptive phenotypic plasticity in cardiac muscle growth is suppressed in high-altitude deer mice. *Evolution* 72(12):2712–2727.
Velotta JP, Jones J, Wolf CJ, Cheviron ZA. 2016. Transcriptomic plasticity in brown adipose tissue contributes to an enhanced capacity for nonshivering thermogenesis in deer mice. *Mol Ecol*. 25(12):2870–2886.
Weir BS, Cockerham CC. 1984. Estimating *F*-statistics for the analysis of population structure. *Evolution* 38(6):1358–1370.
Wu Z, Puigserver P, Andersson U, Zhang C, Adelmant G, Mootha V, Troy A, Cinti S, Lowell B, Scarpulla RC, et al. 1999. Mechanisms controlling mitochondrial biogenesis and respiration through the thermogenic coactivator PGC-1. *Cell* 98(1):115–124.
Yi X, Liang Y, Huerta-Sanchez E, Jin X, Cuo ZXP, Pool JE, Xu X, Jiang H, Vinckenbosch N, Korneliussen TS, et al. 2010. Sequencing of 50 human exomes reveals adaptation to high altitude. *Science* 329:75–78.
Zeng X, Ye M, Resch JM, Jedrychowski MP, Hu B, Lowell BB, Ginty DD, Spiegelman BM. 2019. Innervation of thermogenic adipose tissue via a calsyntenin 3β/S100b axis. *Nature* 569(7755):229–235.
Zhang B, Horvath S. 2005. A general framework for weighted gene co-expression network analysis. *Stat Appl Genet Mol Biol*. 4(1):Article 17.